

Quasi-monolithic GaAs/LiNbO₃/sub 3/-hybrids for acoustoelectric applications

M. Rotter, Achim Wixforth, J. P. Kotthaus, W. Ruile, D. Bernklau, H. Riechert

Angaben zur Veröffentlichung / Publication details:

Rotter, M., Achim Wixforth, J. P. Kotthaus, W. Ruile, D. Bernklau, and H. Riechert. 2002. "Quasi-monolithic GaAs/LiNbO₃/sub 3/-hybrids for acoustoelectric applications." In *1997 IEEE Ultrasonics Symposium Proceedings: An International Symposium, Toronto, ON, Canada, 5-8 October 1997*, edited by S. C. Schneider, M. Levy, and B. R. McAvoy, 201–4. Piscataway, NJ: IEEE. <https://doi.org/10.1109/ultsym.1997.663010>.



Quasi-monolithic GaAs/LiNbO₃-hybrids for acoustoelectric applications

Markus Rotter, Achim Wixforth, and Jörg P. Kotthaus,
Sektion Physik der LMU, Geschwister-Scholl-Platz. 1, D-80539 München, Germany

Werner Ruile, Daniela Bernklau, and Henning Riechert,
Siemens AG, Corporate Technology, D-81730 München, Germany

Abstract — The combination of the electronic properties of a semiconductor heterojunction and the acoustic properties of a piezoelectric material yields very promising surface acoustic wave (SAW) hybrid systems. Quasi-monolithical integration of a thin GaAs/InGaAs/AlGaAs-quantum well structure on a LiNbO₃ SAW device is achieved using the epitaxial lift-off (ELO) technique. The active semiconductor layer system is removed from its substrate and transferred onto the LiNbO₃. The conductivity of the two dimensional electron system in the quantum well, which can be controlled via field effect, modifies the velocity of the surface acoustic waves. Due to the high electromechanical coupling coefficient of LiNbO₃ a change of the electrical boundary conditions produces a large phase shift. This leads to a new class of voltage tunable single-chip SAW devices, e.g., voltage controlled oscillators and tunable SAW delay lines.

1. INTRODUCTION

The propagation velocity of surface acoustic waves on strong piezoelectric materials depends very much on the electric boundary condition: a conductive surface prohibits the effect of piezoelectric stiffening thus reducing the velocity of the surface acoustic wave (SAW). For various applications a continuously tunable velocity would be desirable. Up to now, different approaches were made to combine conventional SAW devices with the electronic properties of semiconductor materials. For example, earlier proposals are based on a space charge zone in a bulk semiconductor that is changing its distance to the surface wave [1,2]. On the other hand, the interaction between surface acoustic waves and a quasi two-dimensional electron system (Q2DES) in semiconductor heterojunctions has recently attracted interest [3,4]. Nevertheless, on most high electron mobility materials, the piezoelectricity is weak, and the effect of the electron system on the SAW is usually small. Therefore quasi-monolithic hybrids with strong piezoelectric substrates

combined with semiconductor layers yield a promising approach to achieve a large tunability of the SAW velocity [5,6].

2. INTERACTION BETWEEN SAW AND Q2DES

The interaction of a SAW and a Q2DES results in a change of SAW velocity $\Delta v/v_0$ and an attenuation Γ of the transmitted SAW intensity $I = I_0 \exp(-\Gamma x)$. This can be described by a simple relaxation model [3]

$$\Gamma = \frac{K_{eff}^2}{2} k \frac{\sigma/\sigma_m}{1 + (\sigma/\sigma_m)^2} \quad (1)$$
$$\frac{\Delta v}{v_0} = \frac{K_{eff}^2}{2} \frac{1}{1 + (\sigma/\sigma_m)^2},$$

where σ is the sheet conductivity and σ_m denotes a critical conductivity where maximum attenuation occurs; K_{eff}^2 is the electromechanical coupling coefficient and $k = 2\pi/\lambda$ is the wave vector of the SAW.

Both, attenuation and velocity change scale with the coupling coefficient K_{eff}^2 . However, in common semiconductor materials the coupling coefficient is very low (i.e., for the GaAs (100) surface: $K_{eff}^2 = 6.4 \times 10^{-4}$). Therefore, the maximum change in SAW velocity is not large enough for most applications. The combination of the electronic properties of GaAs and the strong piezoelectric LiNbO₃ solves this problem. The coupling coefficient of LiNbO₃ (128° rot. YX-cut) is $K_{eff}^2 = 5.6\%$, which is nearly two orders of magnitude higher than on GaAs itself. One approach towards this combination was a sandwichlike structure [7,8], where a GaAs structure was brought into close contact with a LiNbO₃ delay line. A residual gap between the two substrates, however, limits the reproducibility of the coupling between electron system and SAW. Moreover, in this system the sheet conductivity of the Q2DES is not easily tuned.

3. HYBRID TECHNOLOGY

Here, we demonstrate a quasi monolithic hybrid system that can be realized employing the epitaxial lift-off technique (ELO) introduced by Yablonovitch [9,10]: A thin GaAs/AlGaAs-structure is lifted off the growth substrate and can be transferred on nearly arbitrary host substrates. We use an GaAs/AlGaAs/InGaAs-system that is grown by molecular beam epitaxy (MBE). The GaAs substrate is followed by an AlAs layer which is afterwards etched away during the lift-off process. The active layer system consists of modulation-doped $\text{Al}_{0.22}\text{Ga}_{0.78}\text{As}$ -barriers with an embedded $\text{In}_{0.2}\text{Ga}_{0.8}\text{As}$ quantum well. The distance between quantum well and AlAs layer is just 30 nm. After the diffusion of Ohmic contacts to the Q2DES, the structure is covered with a black wax (Apiezon) acting as a stabilizing layer during the ELO process. Then the AlAs-layer is selectively etched away in hydrofluoric acid and the remaining ELO film is transferred onto a LiNbO_3 SAW device (Fig. 1). After some heating procedures this ELO film, which has a thickness of 0.5 μm , is tightly fixed on the LiNbO_3 only by the van-der-Waals-forces. The GaAs film is then patterned and covered by a thin NiCr gate which acts as a field effect electrode.

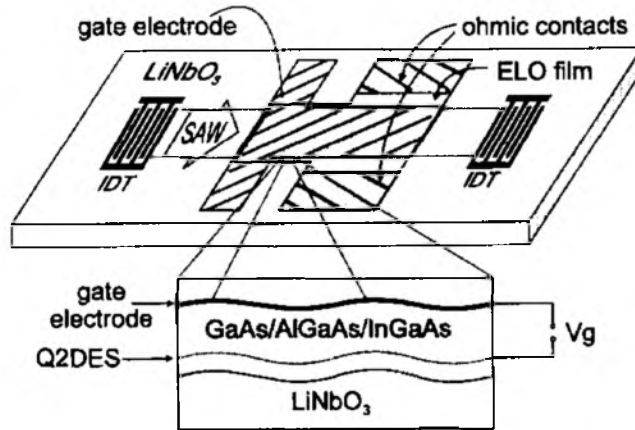


Fig. 1. Schematic sketch of the geometry of a typical hybrid device. Between the gate electrode and the Ohmic contact a negative gate bias is applied. A typical length of the ELO film in the SAW propagation direction is 2 mm.

Detailed investigations on the electronic properties of the ELO films in magnetotransport measurements, photoluminescence, and far infrared spectroscopy at $T = 4.2$ K show no degradation of the Q2DES after the ELO process. Recent work on the epitaxial lift-off technology reveals that mass production of ELO devices could be feasible soon [11].

4. EXPERIMENTAL RESULTS

The ELO film affects the SAW propagation in two different ways: first, it changes the mechanical properties and second, the electrical boundary conditions are modified. The experimentally obtained change of the SAW velocity caused by the mechanical loading of the GaAs film at different excitation frequencies is shown in Fig. 2. The SAW velocity is measured via the delay time of the hybrid system at zero gate bias $V_g = 0$. The effect of the SAW attenuation by the Q2DES can be neglected at $V_g = 0$, because the sheet conductivity σ is large compared to σ_m . As the SAW velocity of GaAs ($v_0 = 2864$ m/s) is much smaller than the corresponding value on LiNbO_3 (128° rot. YX-cut, $v_0 = 3980$ m/s), the layer 'loads' the substrate and therefore the hybrid SAW velocity is lower than on a free LiNbO_3 surface. The SAW velocity decreases with increasing frequency because of the higher ratio between film thickness h and wavelength λ .

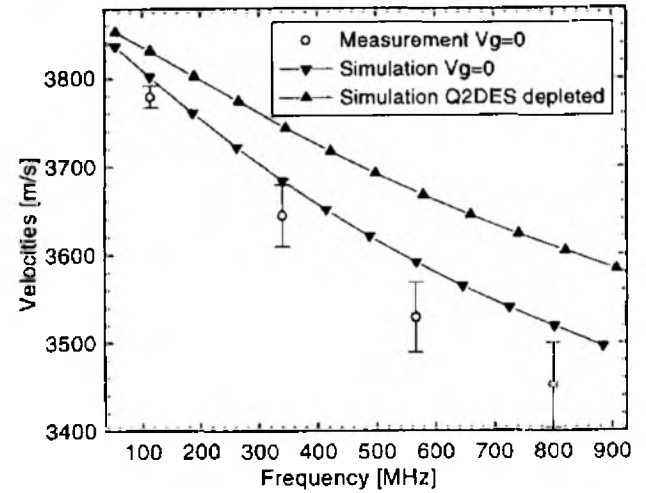


Fig. 2. Measured and calculated SAW propagation velocity at different frequencies in GaAs/ LiNbO_3 hybrids. The error range denotes the standard deviation of the samples.

The velocity is also calculated using a finite element method. Here, the GaAs structure is assumed mechanical homogenous with a conductive layer at the position of the quantum well. Fig. 2 shows the comparison between simulation and experiment.

When a gate voltage is applied to the GaAs system, the carrier density of the Q2DES is reduced and the change in conductivity influences the SAW velocity significantly. In Fig. 2 we also show the simulated velocities when the quantum well is depleted.

Fig. 3 demonstrates the measured velocity change $\Delta v/v$ and the attenuation Γ of the SAW as a function of the gate bias at $f = 340$ MHz. $\Delta v/v$ is calculated from the measured phase shift $\Delta\phi$ via $\frac{\Delta v}{v} = \frac{\Delta\phi}{360^\circ \cdot N}$ where N denotes the number of acoustic wavelengths under the ELO film. Maximum attenuation and maximum differential velocity change occur at $V_g = -5.1$ V where the critical conductivity σ_m is reached. At $V_g = -7$ V the electron system becomes depleted and the remaining conductivity is at such a low level that the electric SAW attenuation is negligible (see Eq. 1). At this low electron concentration the SAW velocity reaches its maximum.

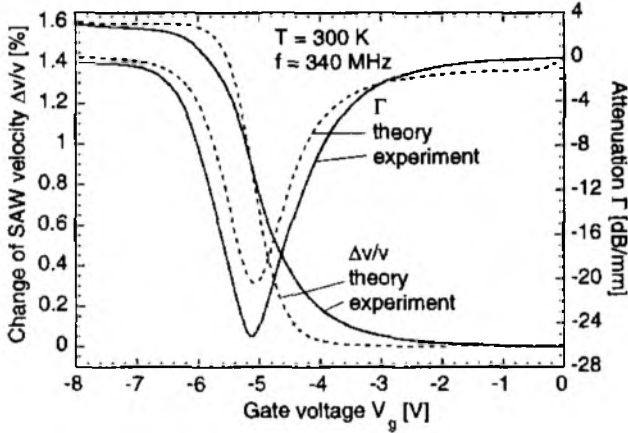


Fig. 3. Change of the SAW velocity and attenuation of the SAW as a function of the voltage between gate and Q2DES.

The sheet conductivity of the same sample was measured in four point geometry. This allows for the comparison between the measured attenuation and velocity change and the relaxation model (Eq. 1). The coupling constant in Eq. 1 has to be replaced by a *hybrid* coupling constant \bar{K}_{eff}^2 . For this constant the acoustic wavelength in comparison to the vertical ELO film layer structure is essential, because the gate electrode screens the SAW potentials at the top of the ELO film, reducing also the potentials at the position of the Q2DES [12]. This leads to a reduction of the hybrid coupling constant compared to the value of free LiNbO_3 . \bar{K}_{eff}^2 can be extracted from the calculated results in Fig. 2: $\bar{K}_{eff}^2 = (v(\text{depleted}) - v(V_g = 0)) / v(\text{depleted})$. For a frequency $f = 340$ MHz the simulations yield a coupling constant of the hybrid $\bar{K}_{eff}^2 = 0.033$ which is 58 % of K_{eff}^2 . The critical conductivity σ_m is approximately given by

$\sigma_m = v\epsilon_0(\sqrt{\epsilon_{xx}\epsilon_{zz}} + 1) = 2.1 \times 10^{-6} \Omega^{-1}$ for $f = 340$ MHz, with ϵ_{xx} and ϵ_{zz} denoting the dielectric constants of LiNbO_3 . These parameters were used to calculate the attenuation and the velocity change of the SAW according to Eq. 1. Fig. 3 demonstrates the good agreement between measurement and the simple relaxation model.

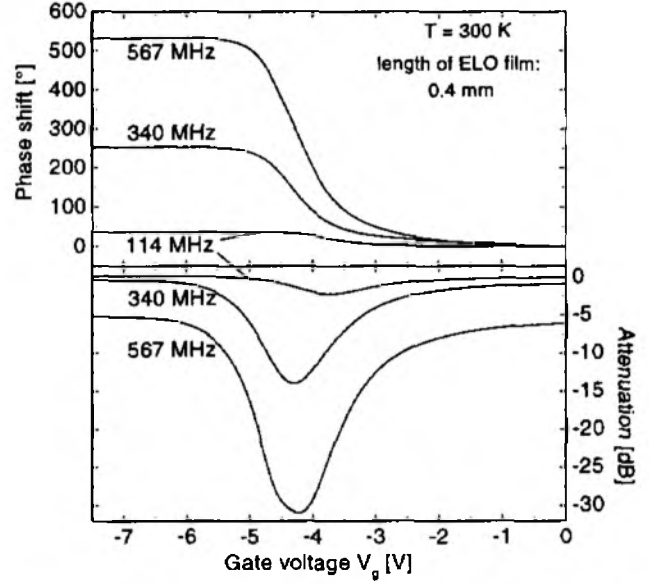


Fig. 4. Phase shift and attenuation of SAW at different frequencies. The insertion losses of the LiNbO_3 structure without ELO film are subtracted.

In Fig. 4 measurements at different frequencies are shown. A split finger transducer geometry is used for the generation of different harmonics in these experiments. Here, the phase shift and the attenuation are displayed for a sample with a ELO film length of 0.4 mm. The insertion losses of the LiNbO_3 device without film are subtracted so that only the mechanical and electrical influence of the ELO film are shown. Mechanically, the GaAs layers lead to an additional attenuation of the surface waves, which is caused by two effects: first, the film produces an attenuation depending on the film length. The second effect is the reflection of the SAW at the edges of the ELO film that act as steps in the acoustic beam path. Both effects depend strongly on the ratio h/λ . Therefore the mechanical SAW attenuation increases with higher frequencies. $\Delta\phi$ as well as Γ increase with smaller wavelength. Fig. 4 also reveals the dependence of \bar{K}_{eff}^2 and σ_m on the wavelength. At a frequency of 114 MHz ($\lambda = 33 \mu\text{m}$) the screening of the SAW potentials at the position of the Q2DES by the gate electrode is very large. Therefore the influence of the conductivity of the electron system on the surface wave is

rather small. With increasing SAW frequency, the hybrid SAW velocity is decreasing, resulting in a reduction of σ_m . This leads to a shift of the points of maximum attenuation towards lower conductivities, i.e. larger negative gate bias.

For applications, a large phase shift is desirable. As $\Delta\phi$ is proportional to the ELO film length, devices with longer films yield larger effects. For samples with a ELO film of 2 mm length a phase shift of 1046° at 340 MHz has been measured. At 434 MHz even a phase shift of 1320° is obtained. This large tuning range of the propagating surface acoustic waves is very interesting for device applications.

5. CONCLUSIONS

LiNbO₃/GaAs hybrid systems fabricated by the epitaxial lift-off technology open a new field for novel tunable SAW devices. Compared to monolithic GaAs SAW devices a velocity change being two orders of magnitude larger is achieved in the hybrid system. With an ELO film of 2 mm length we reach a phase shift of 1320° at $f = 434$ MHz. The experimental results are in good agreement with calculations based on a simple relaxation model. The range of the applied voltage is about 7 V and thus compatible with IC voltages. As the interaction is controlled via field effect, the operation of the device is nearly powerless.

Considering our results a single-chip voltage controlled delay line can be realized. The excellent electronic properties of the GaAs/AlGaAs/InGaAs-heterostructure material allow the integration of rf-amplifiers on the same hybrid chip. This could lead to single-chip voltage controlled oscillators. Also for wireless SAW sensing [13] the hybrid devices are very suitable. Any sensor providing a DC voltage can be read out from a remote location. As the large dynamic electric fields also affect the optical properties of the GaAs structure [6], acoustooptic applications of the hybrids could be possible, too. The excellent acousto-optic properties of LiNbO₃ can be combined with the electro-optic properties of layered GaAs heterojunctions.

6. ACKNOWLEDGMENT

The authors would like to thank S. Manus, T. Ostertag, L. Reindl, S. Berek, and H. Zottl for technical assistance. They gratefully acknowledge fruitful discussions with C. Rocke, A. Tilke, W. Neumayer, U. Rösler, and A. Lorke.

7. REFERENCES

- [1] S. Urabe, *IEEE Trans. Sonics Ultrason.* SU-29, no. 5, 255 (1982)
- [2] J. D. Crowley, J. F. Weller, T. G. Giallorenzi, *Appl. Phys. Lett.* 31, 558 (1977)
- [3] A. Wixforth, J. P. Kotthaus, and G. Weimann, *Phys. Rev.* B40, 7874 (1989)
- [4] R. L. Willet, R. R. Ruel, M. A. Paalanen, K. W. West, and L. N. Pfeiffer, *Phys. Rev.* B47, 7344 (1993)
- [5] K. Hohkawa, H. Suzuki, Q. S. Huang, and S. Noge, *Proc. IEEE Ultrasonic Symp.* 1995, Vol. I, 401
- [6] M. Rotter, C. Rocke, S. Böhm, A. Lorke, A. Wixforth, W. Ruile and L. Korte, *Appl. Phys. Lett.* 70, 2097 (1997)
- [7] A. Wixforth, J. Scriba, M. Wassermeier, J. P. Kotthaus, G. Weimann, and W. Schlapp, *J. Appl. Phys.* 64, 2213 (1988)
- [8] A. Schenstrom, Y. J. Qian, M.-F. Xu, H.-P. Baum, M. Levy und B. K. Sarma, *Solid State Comm.* 65, 739 (1988)
- [9] E. Yablonovitch, T. Gmitter, J. P. Harbison und R. Bhat, *Appl. Phys. Lett.* 51, 2222 (1987)
- [10] E. Yablonovich, D. M. Hwang, T. J. Gmitter, L. T. Florez und J. P. Harbison, *Appl. Phys. Lett.* 56, 2419 (1990)
- [11] see e. g.: P. R. Hageman, G. J. Bauhuis, A. van Geelen, P. C. van Rijsingen, J. J. Schermer, L. J. Giling, *Proc. IEEE PVSC 1996*, 57 (Cat. No. 96CH35897);
J. Maeda, Y. Sasaki, N. Dietz, K. Shibahara, S. Yokoyama, S. Miyazaki, and M. Hirose, *Jpn. J. Appl. Phys.* vol. 36, 1554 (1997)
- [12] C. Rocke, S. Manus und A. Wixforth, *Appl. Phys. Lett.* 65, 2422 (1994)
- [13] L. Reindl, G. Scholl, T. Ostertag, C. C. W. Ruppel, W.-E. Bulst, and F. Seifert, *Proc. IEEE Ultrasonics Symp.* 1996, Vol. I, 363